Effects of twins on the electronic properties of GaAs

Kohei Shimamura,[1,2,3] Zaoshi Yuan,[1,4] Fuyuki Shimojo,[1,2] and Aiichiro Nakano[1]
[1]*Collaboratory for Advanced Computing and Simulations, Department of Physics and Astronomy, Department of Computer Science, Department of Chemical Engineering and Materials Science, University of Southern California, Los Angeles, California 90089-0242, USA*
[2]*Department of Physics, Kumamoto University, Kumamoto 860-8555, Japan*
[3]*Department of Applied Quantum Physics and Nuclear Engineering, Kyushu University, Fukuoka 819-0395, Japan*
[4]*Department of Chemical Engineering, Stanford University, Stanford, California 94305-5025, USA*

(Received 17 May 2013; accepted 4 June 2013; published online 9 July 2013)

Generation of twin defects during the growth of semiconductor nanowires is a major concern, but their effects on electronic properties are not well understood. Here, combined quantum-mechanical and molecular-dynamics simulations reveal that the radiative decay time of an exciton increases due to twin. Furthermore, the twin-scattering contribution to electron mobility is found to be significant, in conformity with photoconductivity measurements. In addition to acting as a carrier-scattering source, twins in nanowires are found to modify the mobility by changing strain and thereby the effective mass. These effects should have profound impacts on the efficiency of nanowire-based devices. © *2013 AIP Publishing LLC*. [http://dx.doi.org/10.1063/1.4811746]

Nanowires (NWs) composed of III-V semiconductors such as gallium arsenide (GaAs) have broad applications[1] including solar cells[2] and vertical transistors.[3] A major problem here is a large number of stacking defects, which may alter electronic properties and degrade device performance.[4] Previous theoretical studies have identified corners and edges on the NW top surface as nucleation sites of stacking defects.[5,6] These defects are thus inherent in NWs. Among various types of stacking defects (e.g., twins and intrinsic/extrinsic stacking faults)[7] are mixed zinc blende (ZB) and wurtzite (WZ) phases for the case of GaAs.[8] Experimental and theoretical studies found profound effects of mixed ZB/WZ phases on the electronic band gap and optical properties.[8] Furthermore, InAs NWs with mixed ZB/WZ phases were found to exhibit 3 times smaller field-effect mobility.[9] However, dominant stacking defects found in III-V NWs are twins,[3,10,11] and how they affect electronic properties are not well understood. Recent advancements in hard X-ray angle-resolved photoemission technology has enabled accurate measurements of electronic band structures in GaAs.[12] With the availability of these new experimental capabilities, it is now timely to assess the effects of twins on electronic properties in GaAs, so as to guide future experiments on this fundamental issue.

Here, combined quantum-mechanical (QM) and molecular-dynamics (MD) simulations are performed to determine the effects of twins on the exciton lifetime and carrier mobility in GaAs. In our QM calculations based on the density functional theory,[13] electronic states are calculated using the projector-augmented-wave method,[14,15] which is an all-electron electronic-structure-calculation method within the frozen-core approximation. The generalized gradient approximation[16] is used for the exchange-correlation energy with non-linear core corrections.[17] The momentum-space formalism is utilized,[18] where the plane-wave cutoff energies are 30 and 250 Ry for the electronic pseudo-wave functions and the pseudo-charge density, respectively. The energy functional is minimized with respect to electronic wave functions iteratively using a preconditioned conjugate-gradient method.[19,20] Projector functions are generated for the 4s, 4p, and 4d states of Ga and As.

We perform QM calculations of GaAs ZB crystal of size $13.85 \times 12.00 \times 78.33$ Å in the x, y, and z directions (which are aligned with the $[1\bar{1}0]$, $[11\bar{2}]$, and [111] crystallographic orientations, respectively). The simulated system contains 288 atoms, and periodic boundary conditions are applied to all Cartesian directions. The Γ point is used for Brillouin zone sampling. We perform two sets of calculations, i.e., with and without twin boundaries; see Fig. 1(a). The [111]-oriented ZB crystalline GaAs is a stack of alternating Ga and As monolayers (MLs), where each ML is a two-dimensional triangular lattice of either Ga or As atoms. According to the lateral positions occupied by the atoms, the triangular lattices are classified into three types: "A," "B," and "C." Let the stacking sequence of the top three As MLs below a (111) plane be ABC, where C is the topmost ML. Then, the next bilayer above the (111) plane consists of a Ga ML in the C triangular lattice followed by an As ML in two possible triangular lattices. Namely, As adatoms without twin defect occupy the A triangular lattice and continue ZB stackings, i.e., ···ABC|ABC···. On the other hand, As atoms with a twin-boundary plane occupy the B triangular lattice and continue to grow as ···ABC|BAC···. In GaAs, radiative band-to-band transitions are dipole allowed, since its conduction and valence bands are s- and p-type, respectively. Thus twin defects could have a major effect on the radiative decay time of an exciton. To estimate the radiative decay time of a bound exciton, we first calculate the oscillator strength[21]

$$f = \frac{2\hbar^2}{mE_{\mathrm{exc}}} \sum_{\alpha} \left| \int d\mathbf{r} \psi_{\mathrm{e}}^{*}(\mathbf{r}) \frac{\nabla \cdot \mathbf{e}}{i} \psi_{\mathrm{h},\alpha}(\mathbf{r}) \right|^2, \qquad (1)$$

where $\hbar$ is Planck's constant, m is the electron mass, E_{exc} is the optical excitation energy, $\mathbf{e}$ is the unit vector parallel to the

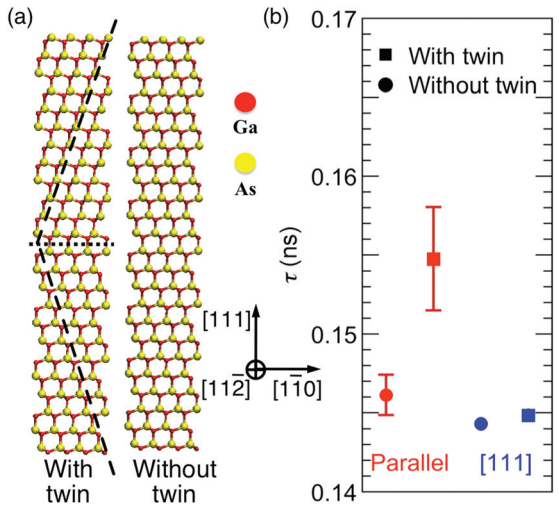

FIG. 1. (a) Simulated GaAs crystal with and without twin boundaries, where red and yellow spheres represent Ga and As atoms, respectively. For the case with twin, the dotted line marks a twin plane, while the dashed lines highlight the change of crystallographic orientations above and below the twin plane. (b) Calculated radiative decay time of a bound exciton without (circles) and with (squares) twins. The red and blue colors are for polarizations parallel and perpendicular to the (111) twin plane, respectively.

polarization of incident light, $\psi_e(\mathbf{r})$ is the electronic wave function at the conduction-band edge, and $\psi_{h,\alpha}(\mathbf{r})$ are the wave functions for the three hole bands (α = heavy, light, and split-off) at the valence-band edge. From the oscillator strength, the radiative decay time for an exciton is calculated as[21]

$$\tau = \frac{2\pi\varepsilon_0 mc^3\hbar^2}{e^2 n E_{exc}^2 f}, \tag{2}$$

where ε_0 is the vacuum permittivity, c is the speed of light, e is the elementary charge, and n is the refractive index.

Figure 1(b) compares the calculated decay times without (circles) and with (squares) twin. The calculated values for polarization parallel to the (111) plane (red color) are averaged over the [1$\bar{1}$0] and [11$\bar{2}$] directions, while the blue color denotes those for [111] polarization. For parallel polarizations, we observe a significant increase of the radiative decay time due to twin. On the other hand, the decay time is not affected much by twin for [111] polarization. The latter may be less affected by the 60° rotation of the crystal around the [111] axis associated with twin. To understand the nature of the transition-dipole integration in Eq. (1), we project $\psi_e(\mathbf{r})$ and $\psi_{h,\alpha}(\mathbf{r})$ onto the wave functions of the pseudoatomic orbitals centered at Ga and As atoms.[22] For the conduction-band edge wave function, $\psi_e(\mathbf{r})$, 67.6% and 32.4% of the total population come from Ga 4s and As 4s states, respectively. The partial populations of the three valence-band edge wave functions, $\psi_{h,\alpha}(\mathbf{r})$, are nearly identical: 80.3% and 11.6%, respectively, from As 4p and Ga 4p states. Namely, the conduction-band wave function is s-like and is centered at Ga atoms, whereas the valence-band wave functions are p-like around As atoms. The transition dipoles thus exist between Ga and As atoms. It should be noted that the calculated radiative decay times here are for bound excitons. For free carriers, in contrary, the radiative lifetime depends on the carrier concentration and is above 1 ns for carrier concentration below 10^{18} cm^{-3}.[23]

The excitonic Bohr radius in GaAs is 115 Å (its binding energy is 4.7 meV), which is larger than the twin-twin distance of 39.165 Å used in the above calculation. The increased lifetime by 6% due to twin in Fig. 1(b) thus corresponds to the case where about 6 twin planes exist within the spread of the excitonic wave function. This is a rather counter-intuitive result, where defects increase the exciton lifetime. It is conceivable that the enhanced charge-recombination lifetime is due to the spatial separation of electron and hole wave functions because of the twin-boundary potential. A similar electron-hole separation has been predicted theoretically for tapered silicon NWs.[24] Experimentally, similar reduction of the oscillator strength was observed in GaN/Al$_x$Ga$_{1-x}$N quantum wells, where the separation of electron and hole wave functions is caused by the piezoelectric field.[25]

Next, we study the effects of twins on carrier mobility. To do so, we first estimate the electronic scattering potential by a twin boundary by subtracting the local Kohn-Sham (KS) potential[26] $v_{KS}(\mathbf{r})$ without twin boundary from that with a twin boundary. Since a twin defect introduces misalignment of atomic positions either above or below the twin-boundary plane, special care must be taken for the subtraction. In our subtraction method, we first sum KS potentials, $v_{KS}^{twin,0^\circ}(\mathbf{r})$ and $v_{KS}^{twin,180^\circ}(\mathbf{r})$, for two systems with twin that are rotated by 180° around the [111] axis from each other (Fig. 2). Similarly, the KS potential without twin is a sum of those in two systems rotated by 180°, $v_{KS}^{ZB,0^\circ}(\mathbf{r})$ and $v_{KS}^{ZB,180^\circ}(\mathbf{r})$ (Fig. 2). These two summed potentials probe KS potentials arising from atoms in exactly the same positions. We can thus subtract the summed KS potential without twin from that with a twin. The resulting electron scattering potential is

$$\Delta v(\mathbf{r}) = \frac{1}{2}\left[\left(v_{KS}^{twin,0^\circ}(\mathbf{r}) + v_{KS}^{twin,180^\circ}(\mathbf{r})\right) - \left(v_{KS}^{ZB,0^\circ}(\mathbf{r}) + v_{KS}^{ZB,180^\circ}(\mathbf{r})\right)\right]. \tag{3}$$

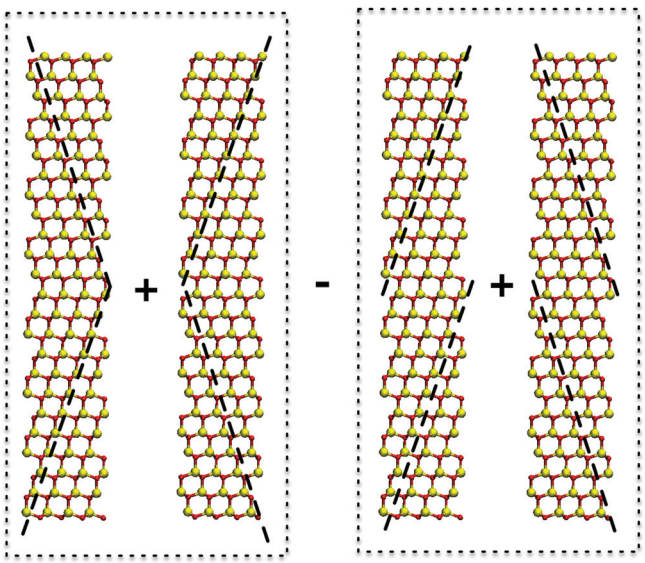

FIG. 2. Subtraction scheme to compute the electron scattering potential due to a twin boundary.

Figure 3(a) shows the calculated electron scattering potential. The scattering potential is a superposition of atom-centered potentials. The side view in Fig. 3(b) superimposed with atomic positions shows that the scattering centers are located on a (111) plane in the middle of Ga (blue) and As (red) monolayers.

We estimate the electron mobility using the electron scattering potential in Fig. 3. In the narrow-wire limit, this can be formulated as a one-dimensional scattering problem.[27] We approximate the scattering potential with height v_0 and range δ through spatial averaging of the potential in Fig. 3 over the x and y directions. We then compute the transmission coefficient as a function of the electron momentum. The electron mean-free path and scattering time are then derived from the transmission coefficient.[27] After thermal average, the final formula for the electron mobility reads

$$\mu = \sqrt{\frac{\pi}{8k_BT}}\frac{e}{m_*^{1/2}}\left[\int dx\, x \ln\left(1+\frac{m_*(v_0\delta)^2}{2\hbar^2 k_B T x^2}\right)e^{-x^2}\right]^{-1} l_{\text{twin}}, \tag{4}$$

where k_B is the Boltzmann constant, T is the temperature, m_* is the electronic effective mass, and l_{twin} is the mean twin-boundary distance. In Eq. (4), x is a dimensionless variable proportional to the electron momentum.

Figure 4 shows the calculated twin-scattering contribution to the electron mobility as a function of the temperature for $l_{\text{twin}} = 1$, 5, and 25 nm. Experimentally, densely populated twin boundaries with a mean distance of a few nm have been observed in GaAs NWs.[3,10] The calculated twin contribution is as low as 10^3 cm^2/(V s) in such a case. This is consistent with recent terahertz photoconductivity measurements by Parkinson *et al.*[4] By eliminating twin defects, they observed the enhancement of the intrinsic carrier mobility from 1200 to 2250 cm^2/(V s) for GaAs NWs of diameter 40–60 nm.[4]

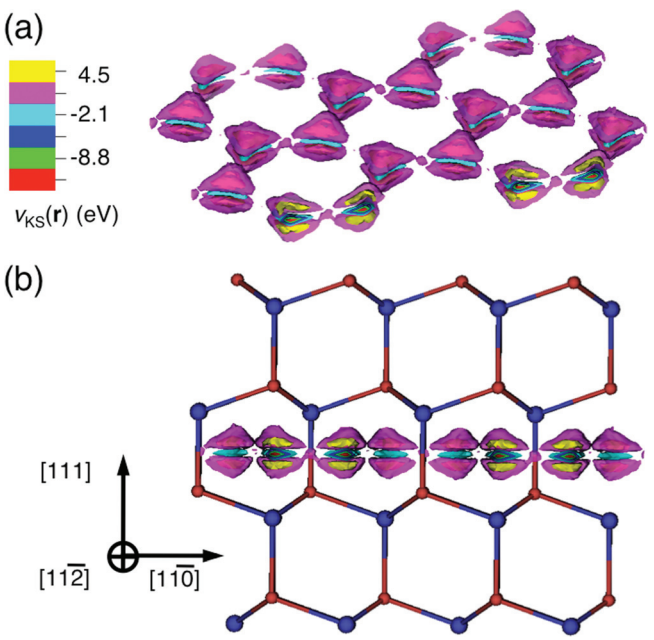

FIG. 3. The electron scattering potential by a twin boundary. (a) Contour plot of the potential. (b) Side view of the potential along with Ga (blue) and As (red) atoms.

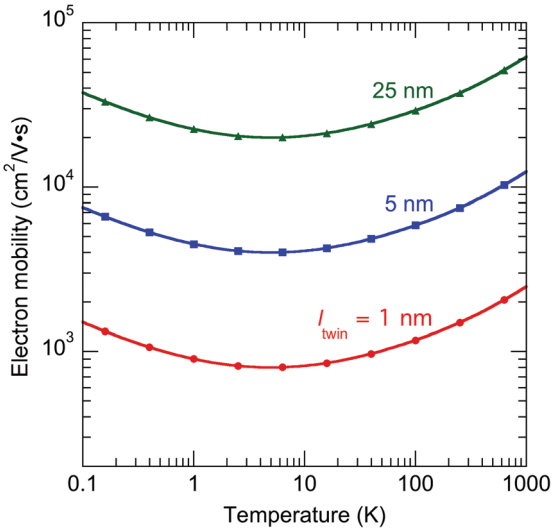

FIG. 4. The calculated twin-scattering contribution to the electron mobility as a function of the temperature for $l_{\text{twin}} = 1$, 5, and 25 nm.

This implies the twin scattering contribution on the order of $\sim 2 \times 10^3$ cm^2/(V s). Here, we should note that the elimination of twin defects in the experiment was achieved by changing growth conditions. According to Parkinson *et al.*, this change in the growth condition may have been accompanied by the reduction of other (e.g., point) defects, and thus the observed mobility change may not reflect solely the twin-scattering contribution.[4] Nevertheless, the present calculation quantitatively supports the interpretation of the mobility enhancement due to twin elimination. Room temperature electron mobilities in high-quality GaAs samples are $\sim 10^4$ cm^2/(V s) (with the corresponding mean free path of $\sim 10^2$ nm), for which the dominant contribution is the scattering by optical phonons.[28] The twin-scattering contribution estimated by the present calculation is more significant for $l_{\text{twin}} < 5$ nm.

In addition to acting as a scattering source for charge carriers, twins affect the electronic property through its effects on strain. This modifies the carrier effective mass, which in turn affects the carrier mobility. To estimate the strain effect, we perform MD simulation of a GaAs NW. The interatomic potential for GaAs[29,30] consists of two- and three-body terms, where the two-body term accounts for steric repulsion as well as Coulombic, charge-dipole, and dipole-dipole interactions, and the three-body term describes bond stretching and bond bending.[31] The interatomic potential has been validated against various experimental and QM calculation results for the lattice constants and cohesive energies of various crystalline phases, elastic constants, surface energies, vibrational density of states, thermal expansion coefficient, specific heat, and melting temperature.[29,30] In particular, the interatomic potential reproduces the contraction of Ga-As bonds near the (110) surface of the ZB crystal, in good agreement with QM results.[6] Such surface relaxation has been shown to be essential for unique thermo-mechanical properties of NWs.[6,32] The simulated GaAs NW has a diameter of 100 Å and height of 500 Å. The wire axis is the [111] orientation of the ZB crystal, and the hexagonal NW has six $\{1\bar{1}0\}$ sidewalls. Periodic boundary condition is

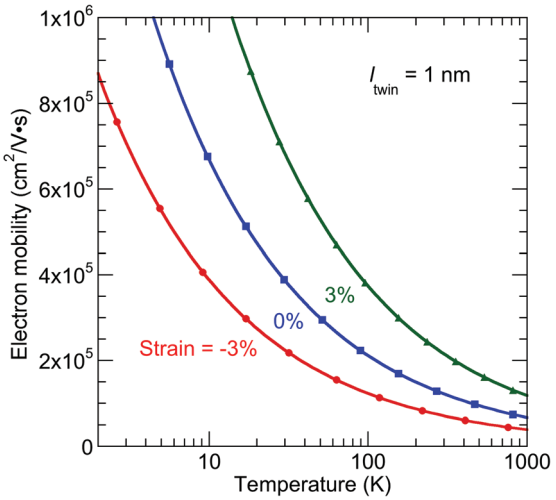

FIG. 5. Twin-scattering contribution to the electron mobility as a function of the temperature for a strain of −3%, 0%, and 3%. The mean twin distance is taken to be 1 nm.

applied to the axial direction. A twin plane is introduced by rotating the upper half of the NW by 60°. The calculated strain distribution reflects the intrinsic core-shell structure previously found in various semiconductor NWs.[6,32] In the shell on the twin-boundary plane, the strain reaches as high as 7%, while in the core region, the strain is 1%–3%.

We estimate the effect of strain tensor $\vec{\vec{\varepsilon}}$ introduced by twin on the electron effective mass m_* using an 8-band k·p model.[33] This model incorporates the dependence of the electronic energy-band structure on strain, polarization, etc. To illustrate the potentially strong dependence of the electron mobility on the strain-dependent effective mass $m_*(\vec{\vec{\varepsilon}})$, we consider a thick-wire limit, where the scattering from different atomic centers at twin boundaries is treated additively. Here, each scattering center is approximated as a spherical impurity potential of height v_0 and radius δ,[28]

$$\mu = \frac{9}{64}\sqrt{\frac{3}{2\pi k_B T}}\frac{e\hbar^4}{[m_*(\vec{\vec{\varepsilon}})]^{5/2}}\left(\frac{a}{v_0\delta^3}\right)^2 l_{\text{twin}}, \qquad (5)$$

where a is the crystalline lattice constant.

Figure 5 shows the calculated electron mobility as a function of the temperature for a hydrostatic strain of −3%, 0%, and 3%. The mean twin distance is taken to be 1 nm. The electron mobility increases by 77% due to 3% (i.e., tensile) strain. On the other hand, it decreases by 42% due to −3% (i.e., compressive) strain. Thus, a few percent of strain modification due to twin results in up to 80% of the mobility change.

In summary, combined QM and MD simulations on GaAs revealed a surprising effect of twin defect, i.e., the radiative decay time of an exciton increases due to twin. Furthermore, the twin-scattering contribution to the electron mobility was estimated as a function of the temperature and twin density. The calculated value is consistent with available photoconductivity measurements. In addition to acting as a carrier-scattering source, twins were found to modify the mobility by changing strain and thereby the effective mass. These effects should be taken into account when discussing the efficiency of NW-based devices.

This work was supported by the U.S. Department of Energy, Office of Science, Office of Basic Energy Sciences under Award DE-SC0001013 as part of the Center for Energy Nanoscience, an Energy Frontier Research Center. Simulations were performed at the Center for High Performance Computing and Communications of the University of Southern California.

[1]Y. B. Wang, H. J. Joyce, Q. A. Gao, X. Z. Liao, H. H. Tan, J. Zou, S. P. Ringer, Z. W. Shan, and C. Jagadish, Nano Lett. **11**(4), 1546–1549 (2011).
[2]J. A. Czaban, D. A. Thompson, and R. R. LaPierre, Nano Lett. **9**(1), 148–154 (2009).
[3]K. Tomioka, M. Yoshimura, and T. Fukui, Nature **488**(7410), 189–192 (2012).
[4]P. Parkinson, H. J. Joyce, Q. Gao, H. H. Tan, X. Zhang, J. Zou, C. Jagadish, L. M. Herz, and M. B. Johnston, Nano Lett. **9**(9), 3349–3353 (2009).
[5]F. Glas, J. C. Harmand, and G. Patriarche, Phys. Rev. Lett. **99**(14), 146101 (2007).
[6]Z. Yuan, K. Nomura, and A. Nakano, Appl. Phys. Lett. **100**(16), 163103 (2012).
[7]F. Glas, J. Appl. Phys. **104**(9), 093520 (2008).
[8]M. Heiss, S. Conesa-Boj, J. Ren, H. H. Tseng, A. Gali, A. Rudolph, E. Uccelli, F. Peiro, J. R. Morante, D. Schuh, E. Reiger, E. Kaxiras, J. Arbiol, and A. F. I. Morral, Phys. Rev. B **83**(4), 045303 (2011).
[9]C. Thelander, P. Caroff, S. Plissard, A. W. Dey, and K. A. Dick, Nano Lett. **11**(6), 2424–2429 (2011).
[10]P. Caroff, K. A. Dick, J. Johansson, M. E. Messing, K. Deppert, and L. Samuelson, Nat. Nanotechnol. **4**(1), 50–55 (2009).
[11]X. Dai, S. A. Dayeh, V. Veeramuthu, A. Larrue, J. Wang, H. B. Su, and C. Soci, Nano Lett. **11**(11), 4947–4952 (2011).
[12]A. X. Gray, C. Papp, S. Ueda, B. Balke, Y. Yamashita, L. Plucinski, J. Minar, J. Braun, E. R. Ylvisaker, C. M. Schneider, W. E. Pickett, H. Ebert, K. Kobayashi, and C. S. Fadley, Nature Mater. **10**(10), 759–764 (2011).
[13]P. Hohenberg and W. Kohn, Phys. Rev. **136**(3B), B864–B871 (1964).
[14]P. E. Blochl, Phys. Rev. B **50**(24), 17953–17979 (1994).
[15]G. Kresse and D. Joubert, Phys. Rev. B **59**(3), 1758–1775 (1999).
[16]J. P. Perdew, K. Burke, and M. Ernzerhof, Phys. Rev. Lett. **77**(18), 3865–3868 (1996).
[17]S. G. Louie, S. Froyen, and M. L. Cohen, Phys. Rev. B **26**(4), 1738–1742 (1982).
[18]J. Ihm, A. Zunger, and M. L. Cohen, J. Phys. C **12**(21), 4409–4422 (1979).
[19]G. Kresse and J. Hafner, Phys. Rev. B **49**(20), 14251–14269 (1994).
[20]F. Shimojo, R. K. Kalia, A. Nakano, and P. Vashishta, Comput. Phys. Commun. **140**(3), 303–314 (2001).
[21]V. A. Fonoberov and A. A. Balandin, J. Appl. Phys. **94**(11), 7178–7186 (2003).
[22]F. Shimojo, A. Nakano, R. K. Kalia, and P. Vashishta, Phys. Rev. E **77**(6), 066103 (2008).
[23]H. C. Casey and F. Stern, J. Appl. Phys. **47**(2), 631–643 (1976).
[24]Z. G. Wu, J. B. Neaton, and J. C. Grossman, Phys. Rev. Lett. **100**(24), 246804 (2008).
[25]J. S. Im, H. Kollmer, J. Off, A. Sohmer, F. Scholz, and A. Hangleiter, Phys. Rev. B **57**(16), R9435–R9438 (1998).
[26]W. Kohn and L. J. Sham, Phys. Rev. **140**(4A), A1133–A1138 (1965).
[27]H. Lee and H. J. Choi, Nano Lett. **10**(6), 2207–2210 (2010).
[28]J. Singh, *Electronic and Optoelectronic Properties of Semiconductor Structures* (Cambridge University Press, Cambridge, UK, 2007).
[29]S. Kodiyalam, R. K. Kalia, H. Kikuchi, A. Nakano, F. Shimojo, and P. Vashishta, Phys. Rev. Lett. **86**(1), 55–58 (2001).
[30]S. Kodiyalam, R. K. Kalia, A. Nakano, and P. Vashishta, Phys. Rev. Lett. **93**(20), 203401 (2004).
[31]P. Vashishta, R. K. Kalia, J. P. Rino, and I. Ebbsjo, Phys. Rev. B **41**(17), 12197–12209 (1990).
[32]Z. Yuan, K. Nomura, and A. Nakano, Appl. Phys. Lett. **100**(15), 153116 (2012).
[33]C. Pryor, Phys. Rev. B **57**(12), 7190–7195 (1998).